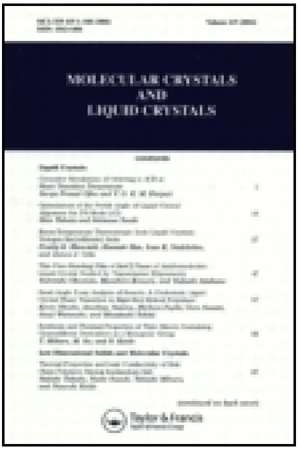

Molecular Crystals and Liquid Crystals
Publication details, including instructions for authors and subscription information:
http://www.tandfonline.com/loi/gmcl16

Characterization of Distortions Induced by a Flow or an Electric Field in Nematic Films Using Conoscopic Experiments

G. Waton [a], A. Ferre [a], S. Candau [a], J. N. Perbet [b] & M. Hareng [b]

[a] Laboratoire d'Acoustique Moléculaire, Université Louis Pasteur, Institut de Physique, 4, rue Blaise Pascal, 67070, Strasbourg, Cedex, France

[b] THOMSON-CSF, Laboratoire Central de Recherches, Domaine de Corbeville, B.P. 10, 91401, Orsay, France

Version of record first published: 14 Oct 2011.

To cite this article: G. Waton , A. Ferre , S. Candau , J. N. Perbet & M. Hareng (1981): Characterization of Distortions Induced by a Flow or an Electric Field in Nematic Films Using Conoscopic Experiments, Molecular Crystals and Liquid Crystals, 78:1, 237-249

To link to this article: http://dx.doi.org/10.1080/00268948108082161

Mol. Cryst. Liq. Cryst., 1981, Vol. 78, pp. 237–249
0026-8941/81/7804-0237 $06.50/0

Printed in the United States of America

Characterization of Distortions Induced by a Flow or an Electric Field in Nematic Films Using Conoscopic Experiments†

G. WATON, A. FERRE, S. CANDAU

Laboratoire d'Acoustique Moléculaire, Université Louis Pasteur, Institut de Physique, 4, rue Blaise Pascal, 67070 Strasbourg Cedex, France

and

J. N. PERBET, M. HARENG

THOMSON-CSF, Laboratoire Central de Recherches, Domaine de Corbeville, B.P. 10, 91401 Orsay, France

(*Received June 4, 1981; in final form July 25, 1981*)

Homeotropic nematic films, distorted under either a Poiseuille flow or a destabilizing electric field have been investigated by means of conoscopic experiments. The experimental patterns are compared with those obtained from a computer procedure. This method allows a determination of the ratio k_{33}/α_2 of the Frank bend elastic constant to the Leslie shear torque coefficient.

INTRODUCTION

Conoscopy is a technique widely applied to the study of distortions of nematic liquid crystal layers.[1] Recently, it was used to characterize the mechanisms involved in the acousto-optical effects observed for nematic liquid crystals.[2,3] These mechanisms involve a streaming of the liquid crystal between two parallel plates, induced by the acoustic radiation pressure.[3] The conoscopic patterns obtained from flow distorted nematic films are rather complex and cannot be computed analytically.

In this paper we present a computer procedure which allows us to calculate

† Work partially supported by D.R.E.T. Contracts n° 78/515 and 78.34/307

conoscopic patterns for several distortion profiles of the optical axis along the normal to the nematic layer. To test the method, the computed patterns are compared with experimental conoscopic figures obtained for homeotropic nematic liquid crystal films distorted either by an electric field or by Poiseuille flow. The latter experiment provides a method of determination of the ratio $|k_{33}/\alpha_2|$ of the Frank bend[4] elastic constant to the Leslie shear torque coefficient.[5]

I NUMERICAL CALCULATION OF CONOSCOPIC PATTERNS OF DISTORTED NEMATIC FILMS

a) Computer procedure

The nematic film is divided into a series of superposed thin layers of thickness δ as shown in the schematic drawing of Figure 1. In each layer, the orientation of the optical axis, defined by a vector **OM** is assumed to be constant but the direction of **OM** is allowed to vary from one layer to another.

Let us consider first a single layer. For a light ray propagating along a direc-

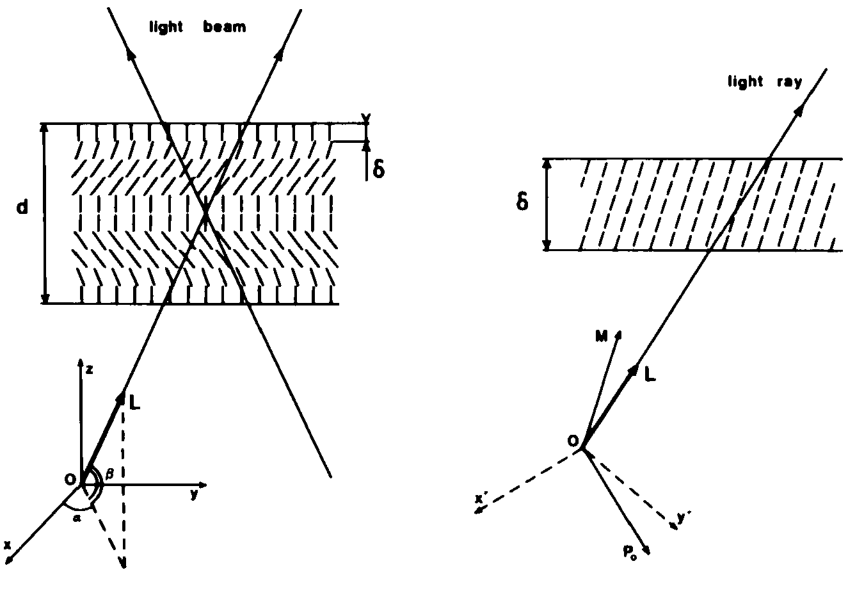

(a) (b)

FIGURE 1 Geometrical parameters.

tion **OL**, the neutral lines **OX** and **OY** are defined through

$$\mathbf{OX} = \mathbf{OL}_\wedge\mathbf{OM}$$
$$\mathbf{OY} = \mathbf{OL}_\wedge(\mathbf{OL}_\wedge\mathbf{OM}) \tag{1}$$

The wave numbers characteristic of waves polarized along **OX** and **OY** are given by:

$$k_X = \frac{2\Pi}{n_o}\lambda_o$$
$$k_Y = \frac{2\Pi}{n_Y}\lambda_o \tag{2}$$

where

$$n_Y = \frac{n_o}{\sqrt{1 + \frac{n_o^2 - n_e^2}{n_o^2}(\mathbf{OL}_\wedge\mathbf{OM})^2}} \tag{3}$$

n_o and n_e are the refractive indices of the ordinary and extraordinary rays respectively, and λ_o is the wavelength of light in a vacuum.[6]

Let $\mathbf{OP}_o$ be the polarization (linear or elliptic) of the light wave falling on the first nematic sublayer, referred to a set of orthogonal coordinates $O_{X'}$, $O_{Y'}$, OL *(cf. Figure 1). The polarization* $\mathbf{OP}_1$ of the light after transmission through the layer is given by:

$$\mathbf{OP}_1 = M\,\mathbf{OP}_o \tag{4}$$

where the transfer matrix M of the layer is:

$$M = C^{-1}\begin{vmatrix} e^{-ik}X_1^\delta & 0 \\ 0 & e^{-ik}Y_1^\delta \end{vmatrix} C \tag{5}$$

and C is the transfer matrix from the coordinate axes O_x, O_y, to the coordinate axes OX_1, OY_1.

The same procedure can be repeated for each layer so that the polarization of the light ray after transmission through n layers can be written as:

$$\mathbf{OP}_n = M_n Mn\text{-}1 \;.\;.\;.\;.\; M_2 M_1\,\mathbf{OP}_o \tag{6}$$

where the subscript n refers to the n^{th} layer.

The light intensity transmitted through an analyzer **OA** is given by:

$$J = |\mathbf{OA}\cdot\mathbf{OP}_n|^2 \tag{7}$$

In order to reconstruct patterns of nematic films illuminated with a convergent light beam, it is necessary to compute J as a function of **OL**. This is done by using an interaction procedure on the cos α, cos β pair, where cos α and cos β are the director cosines in the set of coordinate axes O_x O_y O_z represented in Figure 1. The integration procedure used in the computed program was based on the "Trapezoidal Rule".

The computed patterns were reproduced on graphs by printing a black dot on each point of the field where J exceeds an arbitrarily fixed value.

b) Results

The computer program has been tested on the three types of configurations of the nematic film illustrated on Figure 2. The corresponding conoscopic patterns obtained by the numerical method presented above are reported in Figure 3.

For a homeotropic alignment of the nematic liquid crystal, the computed pattern reproduces the classical maltese cross of a uniaxial crystal cut normal to the optical axis[6] (cf. Figure 3a).

In the second configuration considered here (cf. Figure 2b), the orientation of the optical axis is evenly distorted along the normal to the nematic film, in a

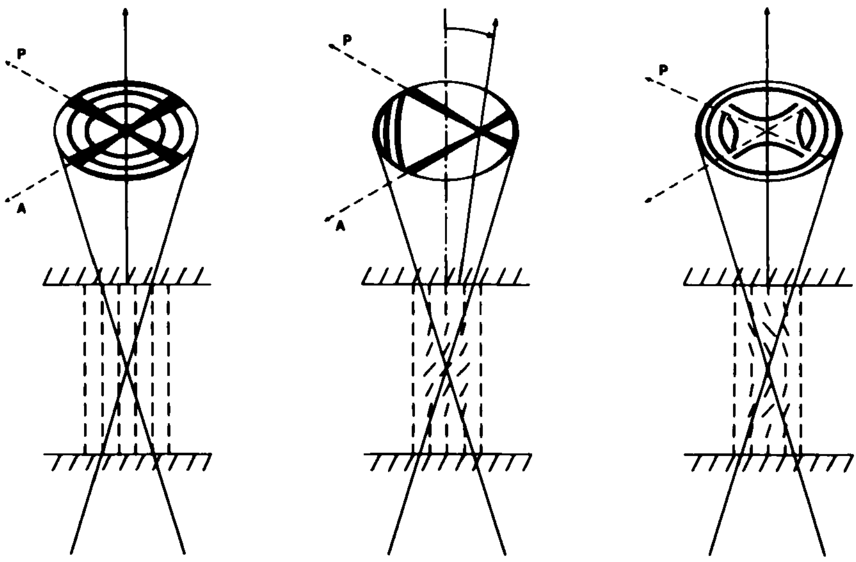

(a) (b) (c)

FIGURE 2 Schematic representation of conoscopic patterns for three orientation profiles of a nematic film. (a) Homeotropic; (b) Even distortion; (c) Odd distortion.

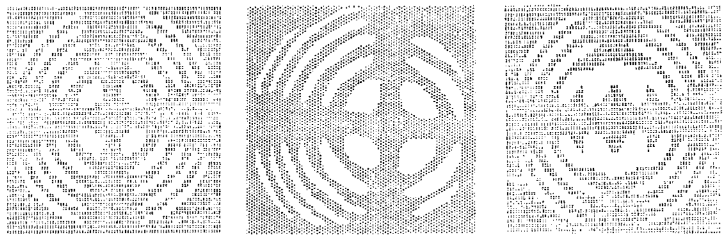

a b c

FIGURE 3 Computed conoscopic patterns for the three profiles represented in Figure 2. (a) Homeotropic; (b) Even distortion ($\theta_o = C^t = 4°$; $d = 150$ μm); (c) Odd distortion ($\theta_o = 3°$; $d = 50$ μm).

given plane. This kind of distortion profile is obtained, for instance, when a destabilizing electric field is applied to the nematic film. In that case, the conoscopic pattern consists of a distorted maltese cross whose center is shifted along the same direction as the optical axis, the shift being proportional to the mean tilt angle. This is indeed observed in Figure 3b which represents the conoscopic pattern computed for the simple configuration when the tilt angle is assumed to be constant across the thickness of the nematic film.

The third investigated configuration corresponds to an odd distortion of the optical axis in a given plane (cf. Figure 2c). The calculation of the conoscopic pattern requires a model for the variation of the tilt angle along the normal Oz to the sample. As we shall see later, the distortion profile relevant to the flow experiments is described by the following variation of the tilt angle θ with z:

$$\theta = \theta_o z\left(\frac{z^2}{(d/2)^2} - 1\right) \tag{7}$$

where θ_o is a constant, d the thickness of the nematic film and $-d/2 \leqslant z \leqslant d/2$.

Figure 3c shows a typical conoscopic pattern computed from Eq. 7. It can be observed that the pattern remains symmetrical with respect to its center.

II EXPERIMENTS ON NEMATIC FILMS DISTORTED BY AN ELECTRIC FIELD

The liquid crystal cell is a thin film (50 μm) of homeotropically aligned liquid crystal sandwiched between two glass plates coated with transparent electrodes. All the measurements are performed at room temperature with ZLI 1085 (Merck) liquid crystal, which has a dielectric anisotropy ($\Delta\epsilon$) of -0.65 at the working frequency (i.e., 10 kHz).

In Figure 4a are shown pictures of the conoscopic patterns obtained for applied voltages equal to 6 Vrms and 8 Vrms respectively. As mentioned before the calculation of the conoscopic pattern requires the knowledge of the distortion profile of the optical area inside the nematic layer. For homeotropic films distorted by an electric field, the tilt angle in the thickness is given by:[7]

$$\theta = \theta_o \cos \frac{\pi z}{d} \tag{8}$$

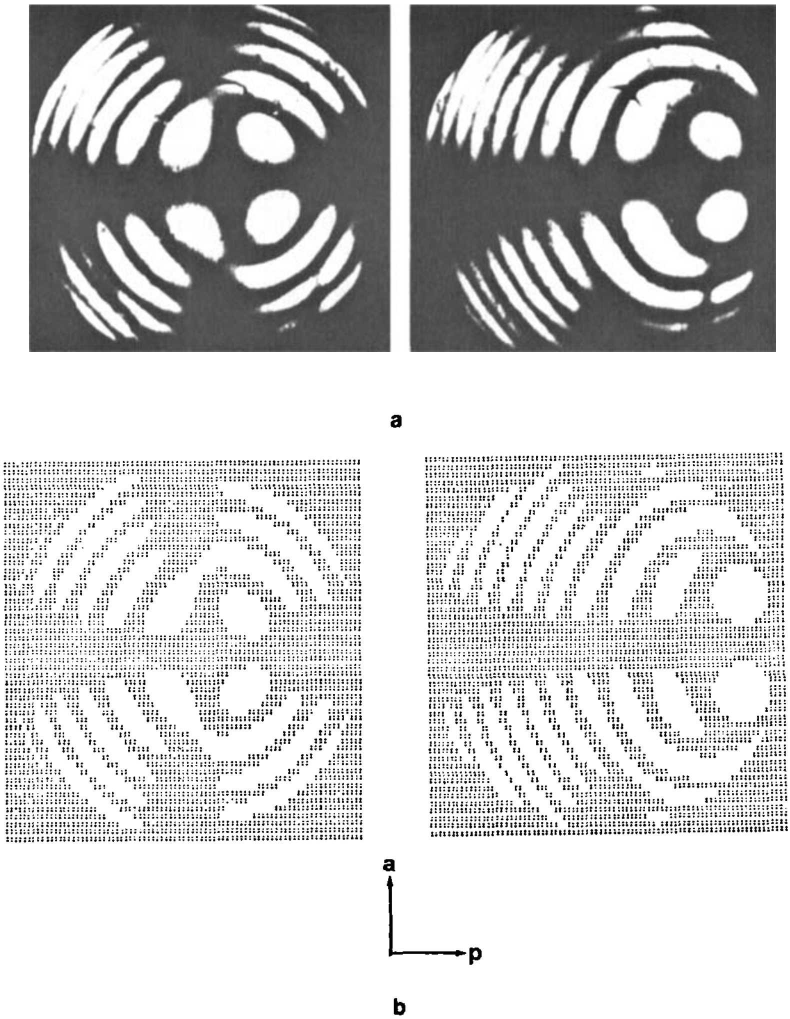

FIGURE 4 Conoscopic patterns for a 50 μm thick homeotropic film of ZLI 1085 nematic liquid crystal under a destabilizing electric field. (a) Experimental patterns; (b) Computed patterns.

Where θ is the local deflection angle, θ_o its amplitude, z the coordinate parallel to the field and L the thickness of the sample extending from $z = -d/2$ to $z = +d/2$.

A set of conoscopic patterns was computed for several values of θ_o using the procedure described earlier. Figure 4b shows the two patterns giving the best fit to the pictures of Figure 4a. The agreement between calculated and experimental patterns is excellent, and the corresponding values of θ_o are:

$$\theta_o = 6^\circ \quad \text{for} \quad V = 6\ V\text{rms}$$

$$\theta_o = 24^\circ \quad \text{for} \quad V = 8\ V\text{rms}$$

The accuracy on the determination of θ_o is approximately $\pm 0.5^\circ$ and is independent of the distortion, so that the relative error $\delta\theta_o/\theta_o$ is inversely proportional to θ_o.

Eventually these angles θ_o can be fitted to the theoretical curve which is given by:

$$\theta_o = \frac{2\sqrt{\dfrac{V}{V_{\text{th}}} - 1}}{\sqrt{\dfrac{k_{11} - k_{33}}{k_{11}} + \dfrac{\epsilon_\perp}{\epsilon_\parallel}}} \quad (\text{when } V \sim V_{\text{th}}) \tag{9}$$

where V_{th} is the threshold voltage and k_{11} is the splay elastic constant. Therefore this method could be used for a very accurate determination of the bend elastic constant k_{33} which is related to V_{th} by the relation:

$$k_{33} = \frac{1}{\pi^2} \cdot \Delta\epsilon \cdot \epsilon_o \cdot V_{\text{th}}^2 \tag{10}$$

III CAPILLARY FLOW EXPERIMENTS

a) Experimental procedure and results

The set-up is shown in Figure 5: the capillary is made of two glass plates, separated with a mylar spacer 50 μm thick. The capillary is filled with 4-cyano-4'-*n*-pentylbiphenyl (5CB). A large aperture microscope lens focuses a polarized light beam onto the sample. A polarizer, crossed with the incident light, causes interferences between the ordinary and extraordinary rays. The interference pattern is then observed on a screen at infinity. After filling, the cell is heated up to the nematic-isotropic transition, then slowly cooled down in order to obtain a good homeotropic alignment. The quality of the alignment is checked by conoscopic observation; the observed pattern is the classical picture with a cross and circles.

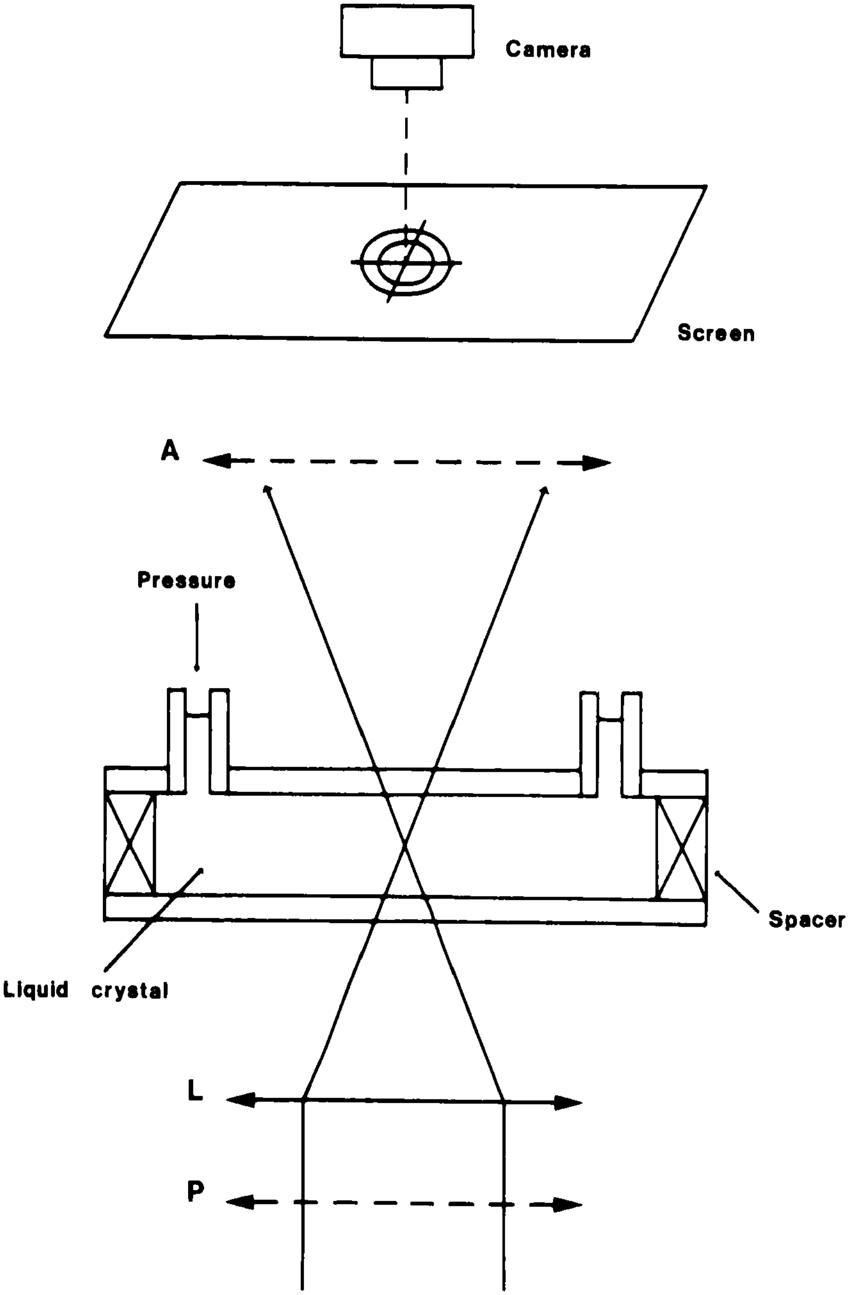

FIGURE 5 Experimental set-up for Poiseuille flow study.

To induce a flow in the capillary, a slight difference of pressure is applied between the two cylindrical glass tubes sealed at the ends of the capillary (cf. Figure 5). The mean flow velocity is obtained from the measurement of the flow rate through one of these tubes.

Photographs 6a and 6d show the conoscopic patterns obtained for several flow velocities and two configurations of the polarizers with respect to the direction of the flow. The interference figure is rather sensitive to the flow velocity but in all cases is symmetrical with respect to its center, which demonstrates the even character of the distortion of the optical axis (cf. Figure 2c).

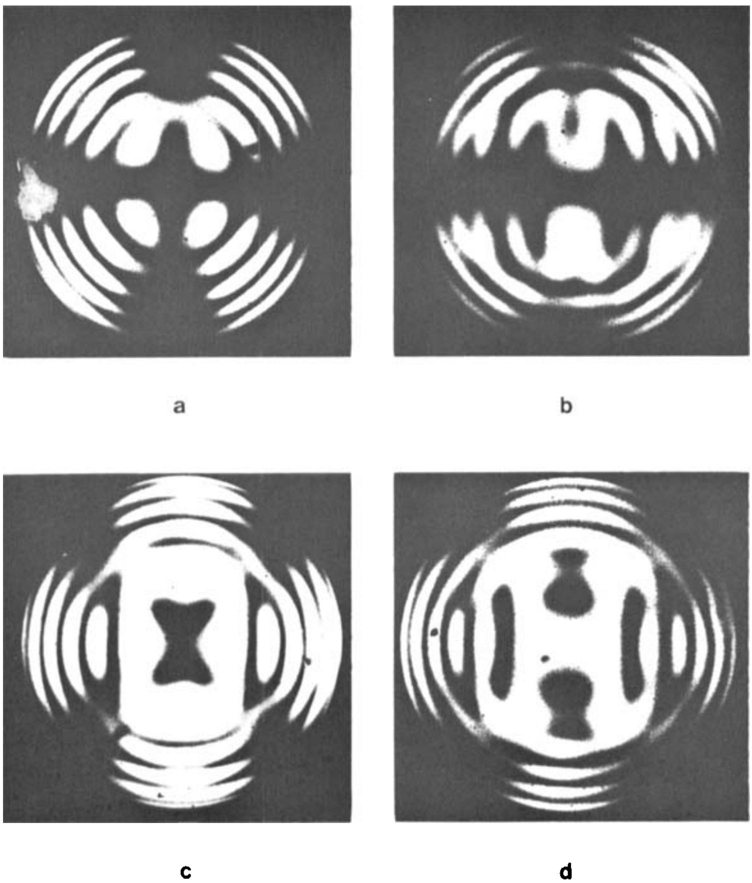

FIGURE 6 Conoscopic patterns obtained for several flow velocities: (a) $u_o = 6$ μm/s; (b) $u_o = 15$ μm/s; (c) $u_o = 6$ μm/s; (d) $u_o = 10.5$ μm/s. (a) and (b) Polarizer parallel to the direction of the flow. (c) and (d) Polarizer at 45° of the direction of the flow.

b) Comparison between experimental and computed patterns

For capillary flow experiments, the distortion profile can be determined from the equation of coupling between flow and director orientation which for small values of the tilt angle $\theta(z)$ and a shear gradient along z can be written as:

$$k_{33} \frac{\delta^2\theta}{\delta z^2} + \alpha_2 \frac{\delta u}{\delta z} = o \qquad (11)$$

where k_{33} is Frank's bend elastic constant, α_2 Leslie's shear torque coefficient and $u = u(z)$ the flow velocity. For Poiseuille flow, $u(z)$ is given by:

$$u(z) = u_o\,(1 - z^2/d/2)^2) \qquad (12)$$

where the origin of the z axis has been taken in the middle of the capillary and u_o is the velocity at $z = o$. Combining Eqs. (11) and (12) yields:

$$\theta = \theta_o z\left(\frac{z^2}{(d/2)^2} - 1\right) \qquad (13)$$

with

$$\theta_o = \frac{\alpha_2 u_o}{3k_{33}} \qquad (14)$$

Then for a given thickness d of the capillary and using Eq. 12, it is possible to calculate conoscopic patterns as a function of θ_o and to compare them with the photographs obtained in flow experiments. This is illustrated on Figure 7 which reproduces computer graphs showing very similar patterns to those reported in Figure 6.

In Figure 8 is reported the variation of θ_o as a function of the velocity u_o as determined rather crudely from the flow rate. The slope of the obtained straight line yields to $|k_{33}/\alpha_2| = 1.8\ 10^{-6}$ dyne p^{-1}. This value is rather close to that determined from a torsional shear flow experiment by Skarp et al. ($k_{33}/\alpha_2 = -10^{-6}$ dyne p^{-1}).[8] It must be noticed that the conoscopic method cannot provide the sign of k_{33}/α_2, since positive and negative tilts are indistinguishable optically.

CONCLUSION

The results reported in this study show that under some circumstances, conoscopic experiments can provide a sensitive and convenient method for the measurement of the deflection of the optical axis of a distorted film of a nematic liquid crystal. This method is based on a comparison between patterns obtained by means of a computer procedure and experimental conoscopic figures. As an illustration, the Poiseuille flow of 5CB nematic liquid crystal

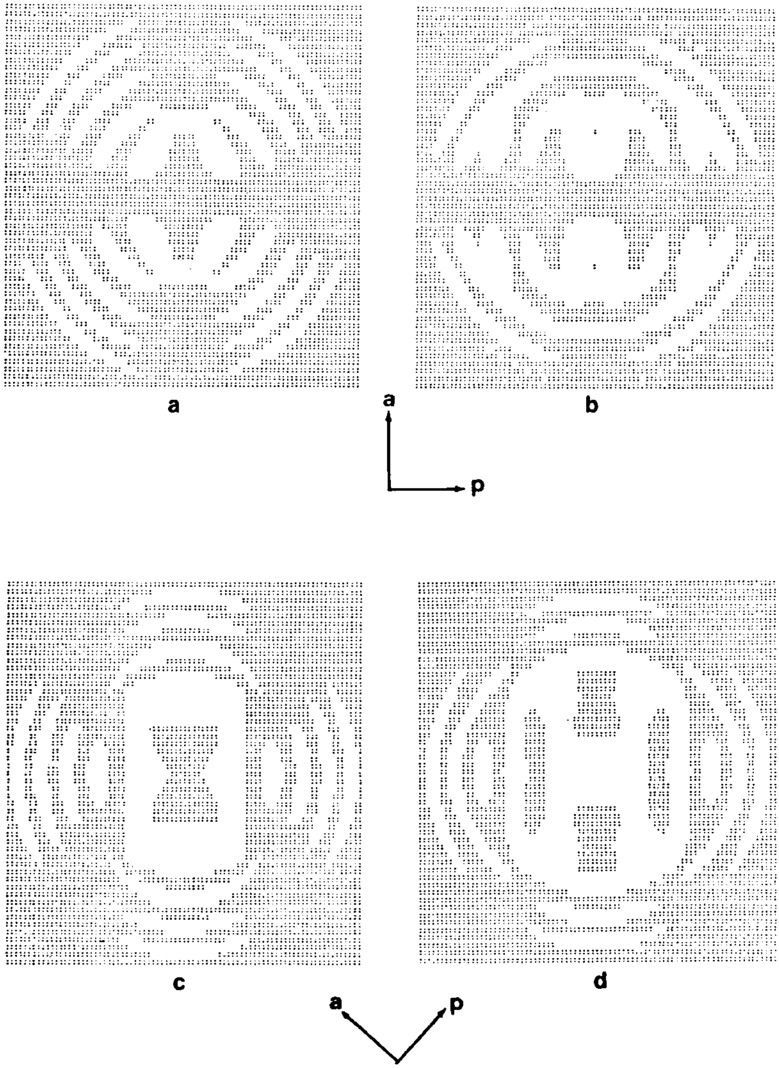

FIGURE 7 Conoscopic patterns computed according to Eq. 7. (a) $\theta_o = 6°$; (b) $\theta_o = 14°5$; (c) $\theta_o = 7°$; (d) $\theta_o = 11°$.

into a rectangular capillary has been investigated. Under flow, the optical axis is tilted with respect to the initial homeotropic orientation in a plane containing the direction of flow and the normal to the capillary. By using the procedure described above, the maximum tilt angle has been determined as a function of the mean velocity, which yields a measurement of the ratio $|k_{33}/\alpha_2|$.

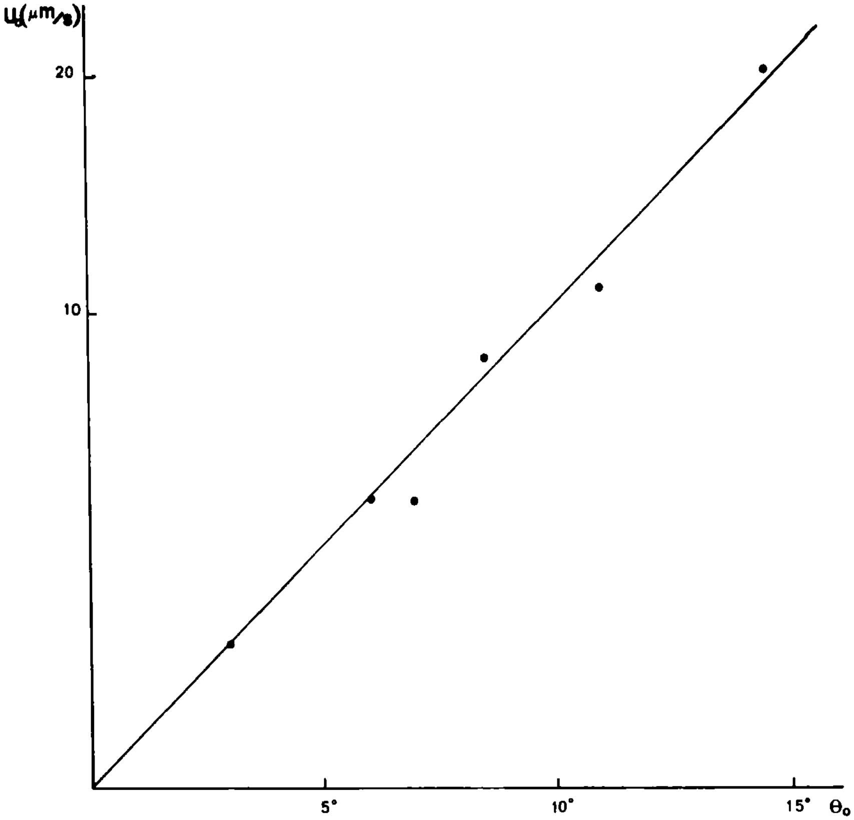

FIGURE 8 Variation of θ_o versus u_o; θ_o has been determined from the comparison between experimental and computed patterns; u_o has been obtained from the mean flow rate.

It must be emphasized that the same method can be applied to other problems involving either electric destabilization or flow of a nematic liquid crystal and more especially acoustical streaming.[3,9,10]

Furthermore, the computer procedure can be easily extended to any kind of distortion of a liquid crystal.

Acknowledgments

The authors wish to thank G. Durand, E. Guyon, and P. Pieranski for very helpful discussions.

References

1. See for instance: P. G. de Gennes, *The Physics of Liquid Crystals*, Oxford University Press, London, 1974.
2. J. N. Perbet and M. Hareng, unpublished results.

3. S. Candau, A. Ferre, A. Peters, G. Waton and P. Pieranski, *Mol. Cryst. Liq. Cryst.*, **61**, 7 (1980).
4. F. C. Frank, *Disc. Faraday. Soc.*, **25**, 19 (1958).
5. F. M. Leslie, *Quart J. Mech. Appl. Math.*, **19**, 357 (1966).
6. See for instance: M. Born and E. Wolf, *Principles of Optics*, Pergamon Press, London, 1970, Chap. XIV.
7. H. Gruler, T. J. Scheffer and G. Meier, *Z Naturforsch*, **27a**, 966 (1972).
8. K. Skarp, S. T. Lagerwall and B. Stebler, *Mol. Cryst. Liq. Cryst.*, **60**, 215 (1980).
9. K. Miyano and Y. R. Shen, *Appl. Phys. Lett.*, **16**, 281 (1976).
10. C. Shripaipan, F. Hayes and T. Fang, *Phys. Rev.*, **A15**, 1297 (1977).